

# Self-Compatibilization of Polymer Blends via Novel Solid-State Shear Extrusion Pulverization

A. R. NESARIKAR,<sup>1</sup> S. H. CARR,<sup>1</sup> K. KHAIT,<sup>1</sup> F. M. MIRABELLA<sup>2</sup>

<sup>1</sup>Department of Materials Science and Engineering and BIRL, Northwestern University, Evanston, Illinois 60208

<sup>2</sup>Process Research Center, Quantum Chemical Company, Morris, Illinois 60450

Received 5 January 1996; accepted 14 May 1996

**ABSTRACT:** The mechanochemistry of a novel economical solid-state shear extrusion (SSSE) pulverization is investigated. SSSE compatibilizes incompatible blends *in situ*; the process has great potential in recycling of post-consumer plastic waste (PCPW). It is proposed that SSSE causes this self-compatibilization of blends by rupturing polymer chains and allowing them to recombine with their neighboring chains. When this recombination involves dissimilar chains at an interface between powder particles, block copolymers are formed, and if the chain transfer reactions are possible, graft copolymers are formed. These copolymers at the interfaces in the phase-separated, incompatible blend lower the interfacial tension and increase the adhesion at the interfaces, thus compatibilizing the blend. Our nuclear magnetic resonance (NMR) and rheology studies reveal the formation of long chain branches (LCBs) in an linear low-density polyethylene (LLDPE), which is equivalent to the formation of graft copolymers in blends. With NMR, an increase from  $\sim 0.2$  to  $\sim 2.0$  of the number of LCBs per 1000 carbon atoms is observed due to pulverization of the LLDPE. © 1997 John Wiley & Sons, Inc. *J Appl Polym Sci* **63**: 1179–1187, 1997

**Key words:** solid-state shear extrusion pulverization; self-compatibilization; polymer blends; nuclear magnetic resonance; rheology

## INTRODUCTION

Post-consumer plastics waste (PCPW) contributes 20% by volume and 8% by weight to the 500 billion pound per year of the municipal solid waste (MSW). PCPW consists of many different plastics or polymers, which could essentially be different chemical compounds altogether and could possess vastly different physical properties and colors. On one hand, it is complex and expensive to sort the individual polymers in the PCPW stream; on the other, if they are recycled in the mixed form, due to their incompatible nature, physical properties

of the final products deteriorate. This mixture is an immiscible polymer blend, in which there is liquid–liquid phase separation in its melt, and the phase separated morphology is preserved in the solid state.<sup>1</sup> If the adhesion at the interfaces between the two phases is poor, which is the case for PCPWs, the interfaces are prone to mechanical failure, and the blend is said to be incompatible. A process that increases the adhesion at the interfaces and the miscibility, thus improving the physical and mechanical properties, is known as compatibilization.

In order to facilitate recycling, efforts are being made in developing economical techniques for the sorting, as well as compatibilizing, of the plastics. Currently, primarily high-density polyethylene (HDPE) and polyethylene terephthalate (PET) are separated from the PCPW stream for recycling; occasionally, sorting of polypropylene (PP), low-

Correspondence to: S. H. Carr.

Contract grant sponsor: Office of Solid Waste Research, Institute for Environmental Studies.

Contract grant number: 13-003.

© 1997 John Wiley & Sons, Inc. CCC 0021-8995/97/091179-09

density polyethylene (LDPE), and other polymers is also seen. However, the remaining unsorted portion of the PCPW stream does pose a big problem, mainly due to unfavorable economics. On the contrary, a successful recycling in the mixed form could handle the entire PCPW stream, provided that one can compatibilize them to improve the physical and mechanical properties of the recycled mixed products. The improvement in the properties is brought about through additives, known as compatibilizers. They, in a phase-separated blend, increase the miscibility to decrease the interfacial area to volume ratio or decrease the interfacial tension to increase the adhesion at the interface; some of them can exhibit both effects. This improves the mechanical properties of the incompatible blends; however, high costs of externally added compatibilizers hamper the economical viability of the process.

A recently suggested<sup>2</sup> novel economical alternative for the compatibilization of the incompatible blends is a solid-state shear extrusion (SSSE) pulverization of the mixed plastics, in which unmelted polymers are subjected to intense shearing action. Low temperatures are maintained throughout the process, minimizing mechanical and oxidative degradation. The SSSE pulverization is thought to compatibilize incompatible polymer blends by *in situ* mechanochemistry.<sup>2</sup> During SSSE, polymer chains rupture, forming free radicals,<sup>2</sup> which are capable of reacting with other chains or free radicals. In blends, this process can lead to formation of block copolymers,<sup>3</sup> and graft copolymers can also be formed if chain transfer reactions are possible. When formed within incompatible blends, these block and graft copolymers travel to the interfaces and position themselves such that their blocks (grafts) reside in the corresponding phases.<sup>4,5</sup> For example, a PP chain segment resides in the PP phase and that of polyethylene (PE) in the PE phase. The presence of block and graft copolymers at the interface reduces the interfacial tension and increases the adhesion at the interfaces between the two phases. Thus, these copolymers act as compatibilizers which are generated *in situ* and improve the physical properties of the incompatible blends. Khait<sup>6</sup> has observed the improvement in the mechanical properties of blends due to the SSSE pulverization, and here we confirm the suggested mechanism for the *in situ* compatibilization.

With application of SSSE in self-compatibilization of mixed PCPW in mind, we study the effectiveness of the self-compatibilization for different

components of the PCPW stream. Currently, we are concentrating on compatibilization of PEs and PP. Here, we discuss and verify the mechanism involved in SSSE. Of the different steps in the mechanism, breaking of chains or formation of free radicals in different polymers is reported by Ahn et al.,<sup>2</sup> where they examined the presence of free radicals with electron spin resonance. However, the formation of free radicals is necessary but not sufficient to generate the block and graft copolymers that result only after successful recombination of the free radicals. Here, we demonstrate a possibility of formation of the copolymers.

SSSE-induced formation of graft copolymers in an incompatible blend of polyethylenes, which undergo chain transfer reactions, is equivalent to a formation of long-chain branches (LCBs) in a single component PE. Therefore, one can verify the creation of LCBs by examining a pulverized polyethylene with nuclear magnetic resonance (NMR) and melt rheology and comparing the results with those of the unpulverized counterpart. Provided the mole fraction of LCBs is significant, one can detect their concentrations. If the unpulverized PE has LCBs, one expects to see an increase in the number of LCBs due to the SSSE pulverization. Details of the two techniques, NMR and rheology, are incorporated in the Discussion section.

Due to the SSSE pulverization, the melt index of a polymer increases as a result of chain rupture.<sup>2</sup> The increase in melt index is an indication of the decrease in the average molecular weight; however, if the free radical chains combine, some of the resulting chains could be longer than the parent chains. The production of both longer and shorter chains during pulverization should broaden the molecular weight distribution. Thus, with an analysis of molecular weight, we can test for a possible decrease in the average molecular weight but an increase in the width of the distribution—observations which would support our proposed explanation of the SSSE mechanism. We will present the effects of SSSE on molecular weight distribution in the next paper.

## EXPERIMENTAL

A linear low-density polyethylene (LLDPE) (Quantum Chemicals Co.), referred to as LL1, was used as provided without any deliberate incorporation of additives and stabilizers. LL1 as virgin resin is called VLL1, and that in the pulverized form is called PLL1. Another LLDPE, called

LL2, was obtained from St. Joseph Plastics (St. Joseph, MO) as the recycled LLDPE. This recycled LLDPE was in the flake form and is expected to have LLDPE of different grades and properties. For testing purposes, LL2 was homogenized by solution precipitation; that is, about half a pound of the mixed flakes were dissolved in a half liter of boiling xylenes, and the polymer was precipitated with ice cold methanol. By this, we expected to either remove or homogenize the different additives and colors. The precipitated recycled LLDPE (LL2) is denoted by RLL2, and its pulverized counterpart by PLL2. LL2 was a recycled LLDPE and was a mixture of different LLDPEs with different colors; it was provided as a mixture of multicolor flakes. However, RLL2, the solution-precipitated sample, had a homogeneous light pink color; and PLL2, the pulverized sample, displayed the same color, which also was equally homogeneous.

Dynamic shear experiments were conducted with a 40 mm diameter cone and plate apparatus in a Bohlin VOR-melt rheometer; cone angle was 2.5 degrees. A frequency range of 0.0314–125.66  $\text{rad s}^{-1}$  was used, and the amplitude of oscillation was maintained at less than 2 mrad. The test samples were molded at about 150°C; precaution was taken so that no air bubbles were left in the final sample. The apparatus was enclosed in an isothermal chamber and heated with hot air. The required gap between the cone and plate was 70  $\mu\text{m}$ , which was adjusted at each temperature to compensate for the thermal expansion or contraction. During the measurements, thermal equilibrium at each temperature was ensured by maintaining the sample at that temperature for more than 20 min before starting the frequency scans. To ensure that no chemical changes took place during measurements, two frequency scans were performed, descending and ascending. Typically, there was a good match between the two data, which eliminated the possibilities of cross-linking and degradation.

For  $^{13}\text{C}$ -NMR, approximately 10% (weight/volume) samples were made in 1,2,4-trichlorobenzene; deuterated benzene was used as the lock solvent; and HMDS (hexamethyldisiloxane) was used as the reference, for which chemical shift is at 2.03 ppm. The measurements were carried out with a Varian Unity-plus-400 NMR with a magnetic field strength of 9.4 tesla. Measurements were made with a 10 mm probe, using 5 mm sample tubes, and by proton signal decoupling. The probe was tuned at 100.577 MHz for  $^{13}\text{C}$  measurements, and over 1000 transitions were accumu-

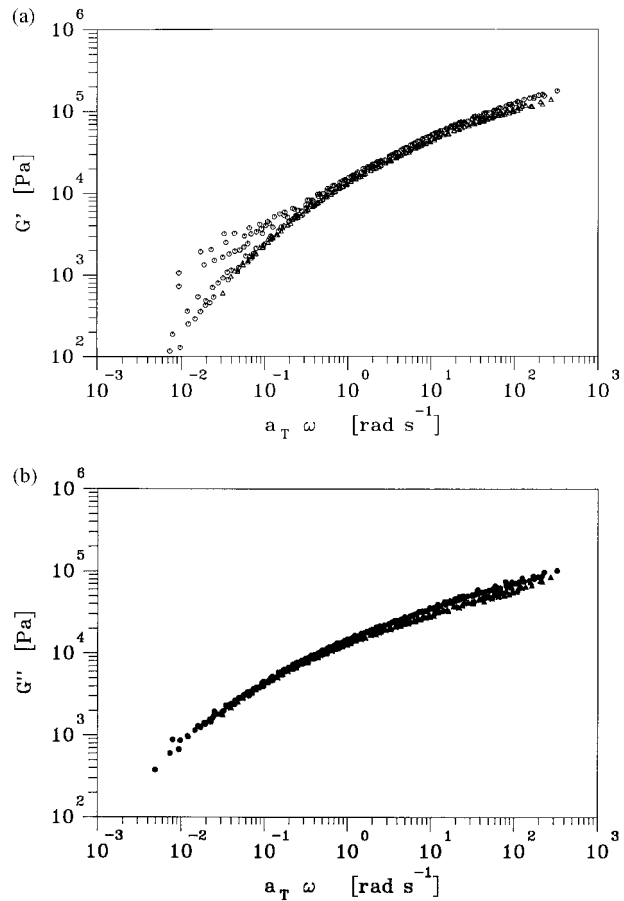


**Figure 1** Superposed rheological data for RLL2 ( $\Delta$ ) and PLL2 ( $\circ$ ). Master curves or reduced curves over a temperature range of 130 to 170°C. The reference temperature  $T_0 = 150^\circ\text{C}$ . (a) Storage modulus ( $G'$ ) versus reduced frequency  $a_T\omega$ . (b) Loss modulus ( $G''$ ) versus reduced frequency  $a_T\omega$ .

lated for every sample. All the experiments were performed at about 120°C. The actual temperature was established by a calibration procedure.

## RESULTS

Figure 1 represents a rheological master curve for RLL2 and PLL2, where  $G'$  [Fig. 1(a)] and  $G''$  [Fig. 1(b)] are the storage and loss moduli, respectively;  $\omega$  is oscillation frequency;  $a_T$  is the horizontal shift factor; the reference temperature  $T_0$  is 150°C. There is a match between  $G''$  of RLL2 and PLL2 [Fig. 1(b)]; however, the  $G'$  values depart from each other for low frequencies [Fig. 1(a)]. Figure 2 shows complex viscosity  $\eta^*$  as a function of oscillation frequency  $\omega$ . There is match between  $\eta^*$  of RLL2 and PLL2 for high frequen-

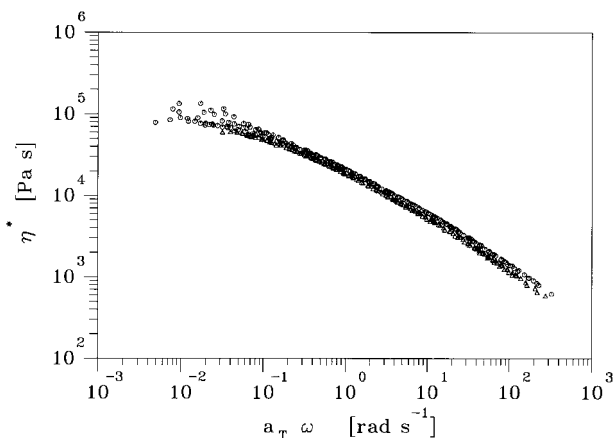


**Figure 2** Complex viscosity ( $\eta^*$ ) versus reduced frequency  $a_T\omega$  over a temperature range of 130 to 170°C, with  $T_0 = 150^\circ\text{C}$ . RLL2 and PLL2 are denoted by  $\Delta$  and  $\circ$ , respectively.

cies, but the match fails in the low frequency range.

A relation between  $a_T$  and temperature  $T$  is shown in Figure 3(a,b). The hollow squares give  $a_T$  values at corresponding temperatures, and the solid line indicates the Arrhenius relation, given by

$$\log a_T = \frac{E_a}{R} [1/T - 1/T_0]$$

Values of  $E_a/R$  for RLL2 and PLL2 are 9334 and 9724 K, respectively, where  $E_a$  and  $R$  are the activation energy and the gas constant. Notice that the fit of the Arrhenius line to the experimental data is satisfactory for both the RLL2 and PLL2 samples.

Master plots or reduced plots for VLL1 and PLL1 are shown in Figure 4(a-c);  $G'$ ,  $G''$ , and  $\eta^*$  are plotted versus  $a_T\omega$  in Figure 4(a-c), respectively. In the low-frequency region, the  $G'$ ,  $G''$ , and  $\eta^*$  parameters distinctly decreased due to pulverization, and they increased in the high-frequency region. The superposition of the curves was done by matching the  $G''$  curves, which successfully superpose. However,  $G'$  and  $\eta^*$  curves for both virgin and pulverized LL1 did not superpose in the low-frequency range. The failure of superposition or the deviations of the curves from each other was larger for pulverized sample than the virgin sample.

Figure 5(a,b) shows the NMR spectra for RLL2 and PLL2, respectively, where the peak intensity is plotted against the ppm for the different spins. These spectra are similar to those obtained by

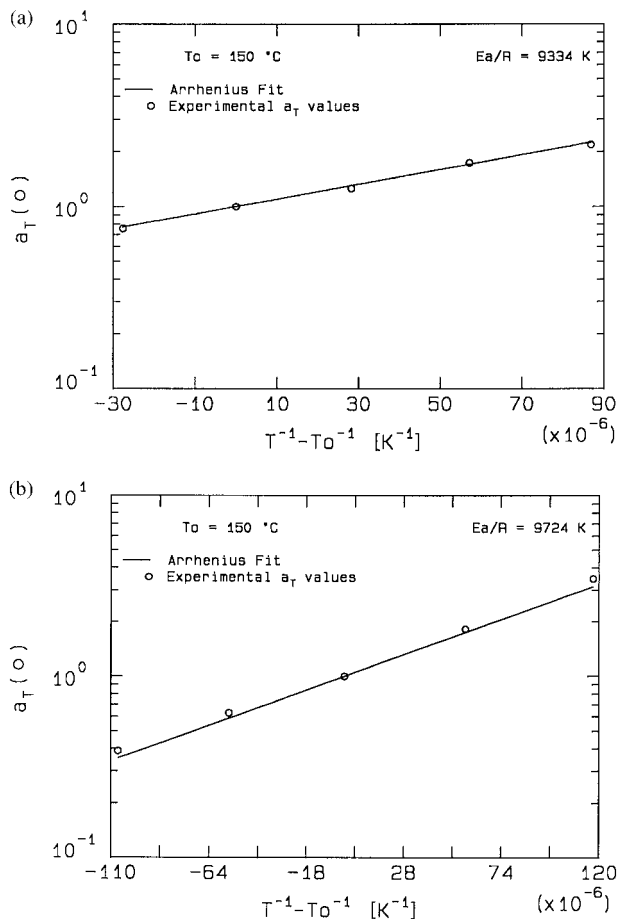


**Figure 3** Best fit of Arrhenius relation to the experimentally obtained values of  $a_T$  versus  $T$ : (a) RLL2 and (b) PLL2.

Randall<sup>7</sup> for LLDPEs. In our spectra, peak widths are narrow, and peak splitting is satisfactory. The improvement in the performance is attributed to the stronger magnetic field due to the superconducting magnets and better double-precision Fourier-transform calculations that come with the advancement in computation.<sup>7</sup>

Similarly, Figure 5(a,b) shows the NMR spectra for VLL1 and PLL1, respectively. The NMR spectra for LL1 are similar to those of LL2 and are not shown here.

## DISCUSSION

Storage modulus  $G'$  is a measure of stored energy (elasticity) of a polymer, and  $G''$  is a measure of energy dissipation (viscosity). The magnitudes of  $G'$  and  $G''$  depend on frequency of oscillation  $\omega$  and the terminal relaxation time  $\tau_t$ . The terminal relaxation time is the minimum time required for

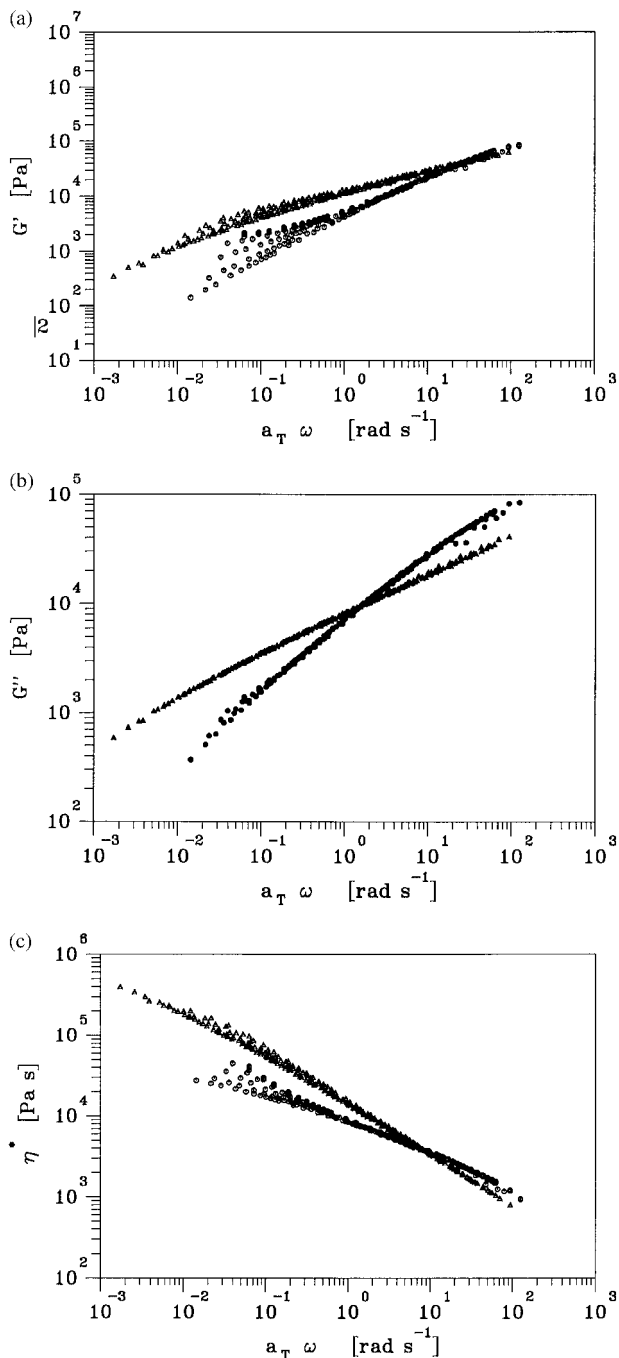


**Figure 4** Superposed rheological data for VLL1 ( $\Delta$ ) and PLL1 ( $\circ$ ). Master curves or reduced curves over a temperature range of 170 to 200°C. The reference temperature  $T_0 = 170^\circ\text{C}$ . (a) Storage modulus ( $G'$ ) versus reduced frequency  $a_T\omega$ . (b) Loss modulus ( $G''$ ) versus reduced frequency  $a_T\omega$ . (c) Complex viscosity ( $\eta^*$ ) versus reduced frequency.

the polymer chains to relax completely, or, in a tube model, is the minimum time for a chain to migrate through a distance equivalent to its contour length. If  $\omega \gg 1/\tau_t$ , the polymer tends to

store the applied energy; thus,  $G' > G''$ . Here, the stretched polymer chains are not given enough time to relax or migrate, which would have caused dissipation of energy. On the other hand, if  $\omega \ll 1/\tau_t$ , dissipation of energy dominates over its storage; thus,  $G'' > G'$ . Here, polymer chains have enough time to relax completely or migrate. In the terminal region ( $\omega \ll 1/\tau_t$ ); for linear monodisperse chains,  $G' \propto \omega^2$  and  $G'' \propto \omega$ ;  $G'$  decreases more rapidly than  $G''$  in the terminal region. However, an introduction of LCBs on the linear chains retards relaxation or migration, and so their  $G'$  is larger than that for the linear chains. An increase in number of LCBs not only increases  $G'$ , but the  $G'$  increase also appears at a higher  $\omega$  value.

In Figure 1(a), we see the characteristic increase in  $G'$  in the terminal region for PLL2. This indicates that there is a minute increase in the number of LCBs in PLL2. Both  $G''$  and zero-shear viscosity,  $\eta_0$  ( $\eta_0 = [G''/\omega]_{\omega \rightarrow 0}$ ), remain unchanged after pulverization, indicating that the degradation of polymer chains during pulverization was minimal. Thus, SSSE created LCBs in the LLDPE without significantly changing its physical properties and processing behavior. Notice that, even for RLL2, we do not see  $G' \propto \omega^2$  and  $G'' \propto \omega$ , which is attributed to its polydispersity in molecular weight.

Also, it was observed that the activation energy ( $E_a$ ) of linear polyethylenes is sensitive to small differences in long-chain branching.<sup>8,9</sup> Movement of linear PE chains is slowed by the long side chains, causing increase in activation energy. Hughes<sup>8</sup> reported  $E_a = 6.0$  kcal/mol for linear systems and 13.5 kcal/mol for systems with excessive long-chain branching. In Bersted's study,<sup>9</sup>  $E_a$  changed from 7.0 to 12.3 kcal/mol when the number of LCBs per 1000 backbone carbon atoms (number of LCBs/1000C) changed from 0.043 to 1.6. In our study,  $E_a$  for RLL2 is 18.55 kcal/mol, and that for PLL2 is 19.32 kcal/mol. If this small increase in activation energy is statistically significant, then it suggests that PLL2 has a few more LCBs than RLL2.

Unlike the recycled LLDPE (LL2), LL1 underwent significant degradation of polymer chains. This is indicated by decreases in  $G''$  and  $\eta^*$  in the low-frequency region due to pulverization [Fig. 4(b,c)]. However, similar to LL2, pulverization increased the deviation of the individual curves from the master curve in the low-frequency region, which is an indication of increased number of LCBs. The small deviations observed in the virgin LL1 may be due to the polydispersity in the

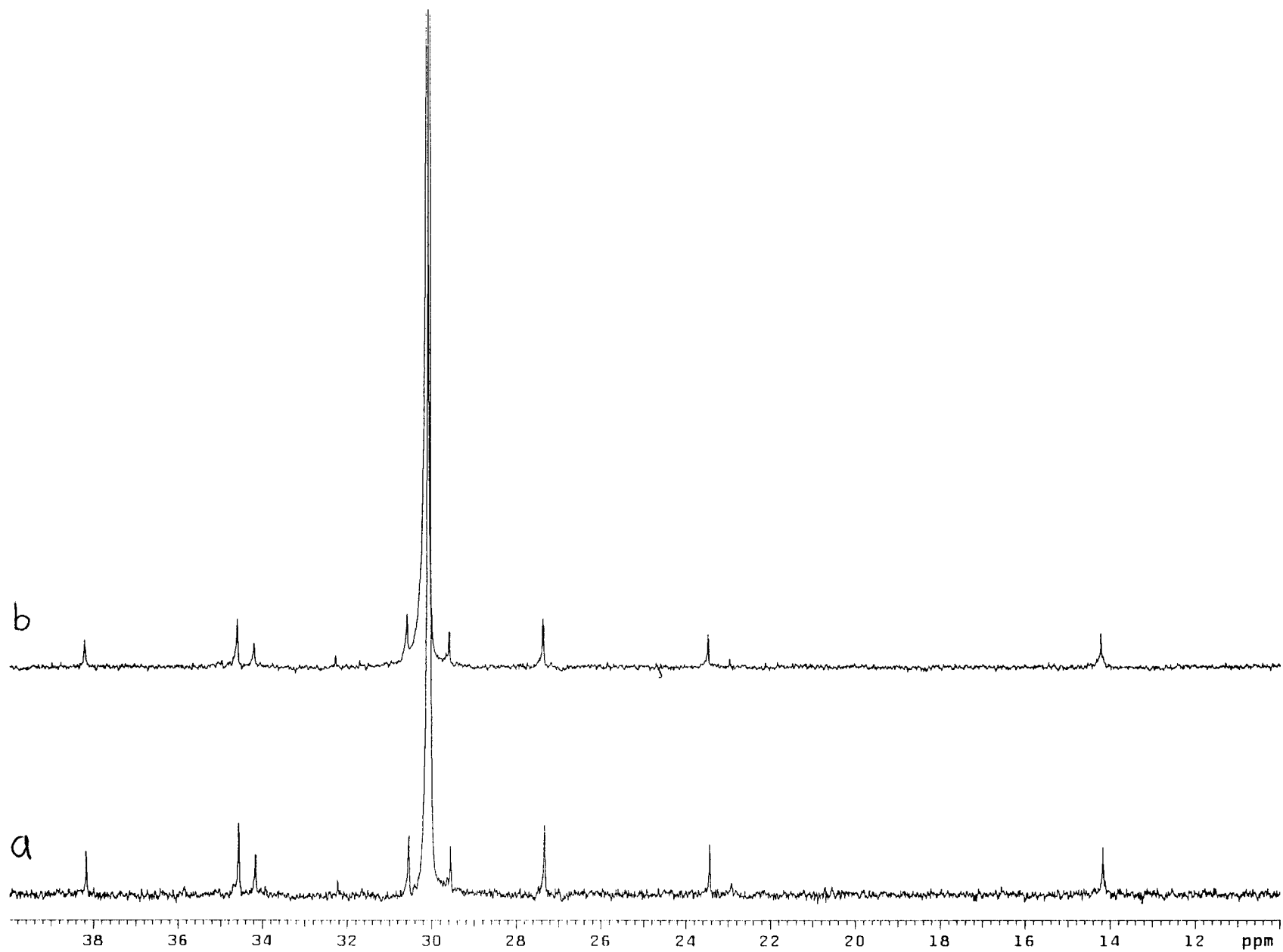


**Figure 5.**  $^{13}\text{C}$  NMR spectra for (a) RLL2 and (b) PLL2;  $\sim 10\%$  (wt/vol) of polymer in 1,2,4-trichlorobenzene was used at  $120^\circ\text{C}$ .

**Table I** Chemical Shifts (in ppm) of Carbon Atoms in a Branched Polyethylene

Branch Length (N)	Methine	$\alpha$	$\beta$	1s	2s	3s	4s	5s	6s
1	33.3	37.6	27.5	20.0					
2	39.7	34.1	27.3	11.2	26.7				
3	37.8	34.4	27.3	14.6	20.3	36.8			
4	38.2	34.6	27.3	14.1	23.4	—	34.2		
5	38.2	34.6	27.3	14.1	22.8	32.8	26.9	34.6	
6	38.2	34.6	27.3	14.1	22.8	32.2	30.4	27.3	34.6

Reproduced from Randall.<sup>7</sup>

molecular weight, which causes failure of time temperature superposition. The reduction in molecular weight of the LL1 due to pulverization decreases  $E_a$ , and the decrease is considerably larger as compared to a possible increase in  $E_a$  due to increased number of LCBs. As expected, there was a decrease in  $E_a/R$ , from 24492 to 10424 K, due to pulverization. Therefore, unlike the LL2 case, change in  $E_a/R$  did not indicate increased number of LCBs, though it was established by increased deviations from the master curve in the terminal region.

The increase in number of LCBs is also noted by NMR analysis. The details of the PE NMR spectra are widely discussed.<sup>7,10-16</sup> Randall<sup>7</sup> explained a method of identifying LCBs on PE chains. He also provided a table of Grant and Paul<sup>17</sup> parameters (see Table I), which predict the chemical shifts for different types of carbons in polyolefins. The nomenclature of different types of carbon atoms in polymer backbone and side chain with  $N$  repeat units are shown in Figure 6.

The NMR spectra of RLL2 [Fig. 5(a)] and PLL2 [Fig. 5(b)] are comparable to an LLDPE spectrum given by Randall.<sup>7</sup> The peaks are representative of chemical shifts, and their positions are given in ppm. Comparisons of different peak ppm with those in the table helps to identify the type of branches that are present in the LLDPE. The backbone methylene carbon atoms give rise to a resonance at  $\sim 30$  ppm, which can affect the peak for  $\gamma$  carbons appearing at 30.4 ppm. A methine peak is present at 38.2 ppm; therefore, we may have  $C_4$ ,  $C_5$ ,  $C_6$ , and LCBs present. Absence of a resonance at 32.8 ppm eliminates the possibility of  $C_5$  branches. The peaks at 34.2 and 32.2 ppm suggest presence of  $C_4$ ,  $C_6$ , and LCBs; the peak at 32.2 also represents the 3s carbon in the chain ends. LLDPEs are predominantly copolymers of hexene-1; therefore, they have substantial branches with four carbon atoms ( $C_4$  branches). Also, we assume that short-chain branches having six or more carbon atoms ( $C_6$ ,  $C_7$ ,  $C_8$ , etc.) are present in insignificantly small

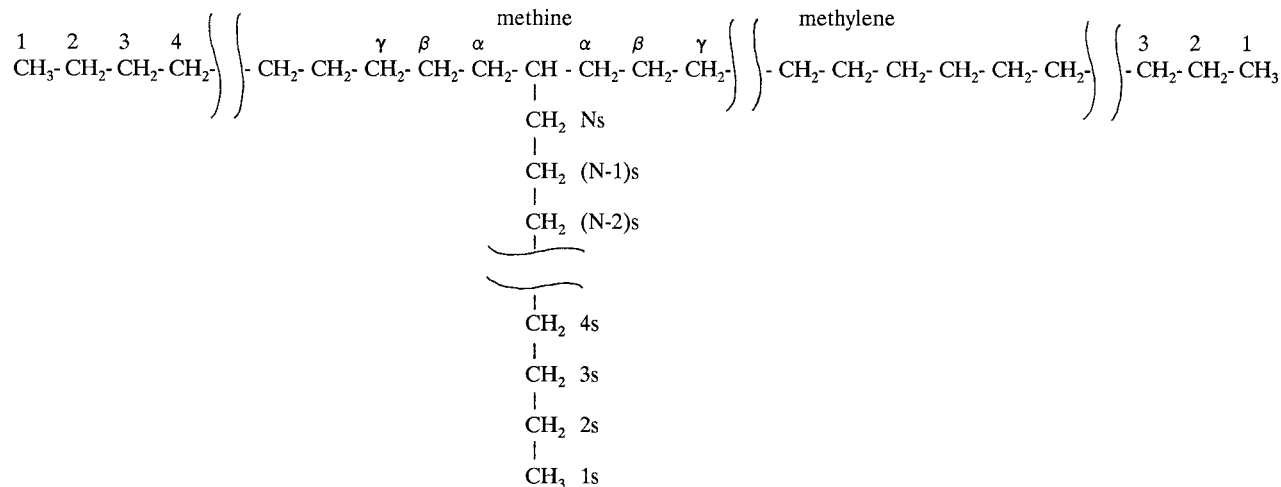


**Figure 6** Nomenclature of different carbon atoms in polymer backbone and a side chain with  $N$  carbon atoms.

**Table II Concentrations of Butyl ( $C_4$ ) and Long-chain Branches as Calculated from the NMR Spectra**

Linear Low-density Polyethylenes	Number of Butyl Branches Per 1000 Backbone Carbon Atoms ( $m$ )	Number of LCBs per 1000 Backbone Carbon Atoms ( $n$ )
RLL2	15.2	0.2
PLL2	18.3	1.8
VLL1	18.3	0.2
PLL1	17.3	2.4

numbers. This assumption is supported by the measurement of short-chain-branching distribution by temperature rising elution fractionation (TREF). The TREF distributions of virgin and pulverized samples of LLDPEs were identical. Thus, peaks at 32.2 and 22.8 ppm represent chain ends and, if their concentration is significant, LCBs.

An accurate qualitative analysis by NMR requires use of adequate relaxation time between consecutive transitions for a long-term data averaging. However, spin-lattice relaxation times ( $T_{1s}$ ) for 1s (methyl) carbons can range from three to seven seconds,<sup>18</sup> so one is required to allow five times that (about 30s) as the time between transitions. That enormously increases the time for large enough number of transitions to obtain an acceptable signal-to-noise ratio. A solution to the problem, as suggested by Randall,<sup>7</sup> is to concentrate on only those peaks that have small and comparable  $T_{1s}$ . Since,  $T_{1s}$  for 4s in  $C_4$  (34.4 ppm) and  $\alpha$  carbon atoms (34.6 ppm) are small and similar,<sup>18</sup> we concentrate on their peaks to determine concentrations of  $C_4$  and LCBs. NMR has a distinct advantage over other techniques (namely, infrared), as the proportionality constant relating the area under a peak to the concentration of its contributing carbon atom is the same for all the types of carbon atoms.

Thus, to determine concentrations of  $C_4$  and LCBs, consider an LLDPE with  $n$  number of LCBs and  $m$  number of  $C_4$  branches per 1000 backbone carbon atoms. As there is one 4s carbon per butyl branch, the area of the 4s peak at 34.4 ppm will be proportional to  $m$ . There are two  $\alpha$ -C in  $C_4$  branches and three in LCBs; therefore, the area under the  $\alpha$ -C peak at 34.6 ppm will be proportional to  $2m + 3n$ . If LCBs are absent (i.e.,  $n = 0$ ), the contribution of  $\alpha$ -C ( $\propto 2m$ ) is double that of 4-C ( $\propto m$ ). Thus, if the area under the methylene peak at 30 ppm is 1000 units, then the areas under the  $\alpha$  and 4s peaks are  $2m + 3n$  and  $m$ , respec-

tively. The values of  $m$  and  $n$  can be calculated as shown in Table II.

The NMR spectra for LL1 were similar to those of LL2 and are not shown here. Also, the number of butyl branches was independently determined by NMR in Quantum Chemical Inc. to be 17.8, which is in good agreement with our value. They also performed TREF analysis on VLL1 and PLL1. There was a good match between the TREF curves of VLL1 and PLL1. Thus, by TREF, not only that the average number of short-chain branching was observed to be constant, but their distributions were seen to be unchanged. Also, in our data (Table II), the difference in values of  $m$  for LL2 are the same within experimental error, and one concludes that the pulverization did not alter concentrations of butyl branches. On the other hand, values of  $n$  (number of LCBs) systematically increased due to the pulverization. Both the unpulverized LLDPEs showed almost no LCBs, but their pulverized counterparts have finite LCBs.

The concentration of LCBs is about 2 per 1000 backbone carbon atoms. A comparable concentration of graft copolymers is expected to be generated by the SSSE pulverization in an incompatible blend. The actual concentration of graft copolymers will be less, as some of the free radicals will attach to polymers chains of the same kind producing long-chain branches. However, in blends, block copolymers will also be produced.

To understand the effectiveness of this copolymer concentration in self-compatibilization of the blend, consider a concentration of 1 graft per 1000 backbone carbon atoms in a pulverized blend, which means, for a polymer with an  $M_n$  of 14,000 (i.e., an average of 1000 carbon atoms per chain), an average chain will have a graft on it. Moreover, this graft copolymer concentration is supplemented by block copolymers. Almost every polymer chain in the blend is a copolymer of the two blend components. This is an ideal condition for



compatibilization of the blend. Even if the concentration of the copolymer is small and is equivalent to that when the blend is compatibilized by externally added copolymer, mixing of the former is on the submolecular level as opposed to the later, in which compatibilizing agents are added to the incompatible blend by mechanical means. *In situ* formation of the copolymers in the SSSE pulverization assures a thorough mixing of the copolymers, which is vital for them to travel to the interfaces and reside there. Thorough mixing of the SSSE pulverization is indicated by the homogeneous color of the pulverized product, even though the feedstock consisted of multicolor flakes. The homogeneous light pink color of the solution precipitated sample, RLL2, was also exhibited by the pulverized sample.

## CONCLUSIONS

The results of the critical experiments reported in the preceding are what one would expect if the proposed mechanism of self-compatibilization by the SSSE pulverization is correct; namely, the chains rupture forming free radicals, and the free radicals rejoin to form graft and block copolymers. We verified the rejoining of the free radicals during the SSSE pulverization by examining a recycled and a virgin LLDPE. After SSSE pulverization, a detectable concentration of long-chain branches, which are equivalent to graft copolymers in blends, were formed.

Increase in the number of LCBs due to pulverization increased the activation energy ( $E_a$ ) of the recycled LLDPE (LL2) from 18.6 to 19.3 kcal/mol and increased the storage modulus in the terminal region. However, the zero-shear viscosity was unaffected by pulverization; that is, the pulverization did not alter the molecular weight of LL2. On the other hand, a substantial decrease was observed in the molecular weight of LL1, causing a decrease in  $G'$ ,  $G''$ , and  $\eta^*$  in the terminal region and  $E_a$ . However, the increased deviations from the master curve in the terminal region confirmed an increased number of LCBs.

The long- and short-chain C4 were detected, and their concentrations were measured by NMR.

TREF analysis confirmed our NMR result that there was no change in short-chain branching average concentration. It also showed no change in the short-chain branching distribution curves due to pulverization. However, our NMR data established that the concentration of LCBs per 1000 backbone carbon atoms rose from  $\sim 0.2$  to  $\sim 2$  in the pulverized recycled and virgin LLDPEs.

The authors thank Richard Kwarcinski and John Rasmussen for SSSE pulverizing the LLDPEs used in this work.

## REFERENCES

1. A. R. Nesarikar, PhD Thesis, Northwestern University, Evanston, IL, 1994.
2. D. Ahn, K. Khait, and M. Petrich, *J. Appl. Polym. Sci.*, **55**, 1431 (1995).
3. A. Casale and R. S. Porter, *Polymer Stress Reactions*, Academic Press, New York, 1978.
4. D. R. Paul, in *Polymer Blends*, Vol. 2, D. R. Paul and S. Newman, Eds., Academic Press, New York, 1978, Chap. 12.
5. R. J. Roe, and C. M. Kuo, *Macromolecules*, **23**, 4635 (1990).
6. K. Khait, *Proceedings of SPE, 53rd ANTEC*, Boston, MA, Vol. 53, 1995, p. 2066.
7. J. C. Randall, in *Polymer Characterization by ESR and NMR*, A. E. Woodward and F. A. Bovey, Eds., ACS Symposium Series 142, 1980, Chap. 6.
8. J. K. Hughes, *SPE Antec Tech. Papers*, **29**, 306 (1983).
9. B. H. Bersted, *J. Appl. Polym. Sci.*, **30**, 3751 (1985).
10. D. E. Dorman, E. P. Otocka, and F. A. Bovey, *Macromolecules*, **5**, 574 (1972).
11. J. C. Randall, *J. Polym. Sci., Polym. Phys. Ed.*, **11**, 275 (1973).
12. D. E. Axelson, G. C. Levy, and L. Mandelkern, *Macromolecules*, **12**, 41 (1979).
13. M. E. A. Cudby and A. Bunn, *Polymer*, **17**, 345 (1976).
14. J. C. Randall, *J. Appl. Polym. Sci.*, **22**, 585 (1978).
15. F. A. Bovey, F. C. Schilling, F. L. McCrackin, and H. L. Wagner, *Macromolecules*, **9**, 76 (1976).
16. G. N. Foster, *Polym. Prepr.*, **20**, 463 (1979).
17. D. M. Grant and E. G. Paul, *J. Amer. Chem. Soc.*, **86**, 2984 (1964).
18. D. E. Axelson, L. Mandelkern, and G. C. Levy, *Macromolecules*, **10**, 557 (1977).